Published in final edited form as:
BJU Int. 2008 December ; 102(11): 1681–1686. doi:10.1111/j.1464-410X.2008.07896.x.

Effect of Firing Rate on the Performance of Shock Wave Lithotriptors

Yuri A. Pishchalnikov, **James A. McAteer**, and **James C. Williams Jr.**
Department of Anatomy and Cell Biology, Indiana University School of Medicine, Indianapolis, Indiana

Abstract

Objective—To determine the mechanism that underlies the effect of shock wave (SW) rate on the performance of clinical lithotripters.

Materials and Methods—The effect of firing rate on the pressure characteristics of SWs was assessed using a fiber-optic probe hydrophone (FOPH 500, RP Acoustics, Leutenbach, Germany). Shock waves were fired at slow (5−27 SW/min) and fast (100−120 SW/min) rates using a conventional high-pressure lithotriptor (DoLi-50, Dornier MedTech America, Inc., Kennesaw, GA, USA), and a new low-pressure lithotriptor (XX-ES, Xi Xin Medical Instruments Co. Ltd, Suzhou, PRC). A digital camcorder (HDR-HC3, Sony, Japan) was used to record cavitation fields, and an ultrafast multiframe high-speed camera (Imacon 200, DRS Data & Imaging Systems, Inc., Oakland, NJ, USA) was used to follow the evolution of bubbles throughout the cavitation cycle.

Results—Firing rate had little effect on the leading positive-pressure phase of the SWs with the DoLi lithotriptor. A slight reduction (~7%) of peak positive pressure (P +) was detected only in the very dense cavitation fields (~1000 bubbles/cm^3) generated at the fastest firing rate (120 SW/min) in nondegassed water. The negative pressure of the SWs, on the other hand, was dramatically affected by firing rate. At 120 SW/min the peak negative pressure was reduced by ~84%, the duration and area of the negative pressure component was reduced by ~80% and ~98%, respectively, and the energy density of negative pressure was reduced by > 99%. Whereas cavitation bubbles proliferated at fast firing rates, HS-camera images showed the bubbles that persisted between SWs were very small (< 10 μm). Similar results were obtained with the XX-ES lithotriptor but only after recognizing a rate-dependent charging artefact with that machine.

Conclusion—Increasing the firing rate of a lithotriptor can dramatically reduce the negative pressure component of the SWs, while the positive pressure remains virtually unaffected. Cavitation increases as the firing rate is increased but as the bubbles collapse, they break into numerous microbubbles that, because of their very small size, do not pose a barrier to the leading positive pressure of the next SW. These findings begin to explain why stone breakage in SWL becomes less efficient as the firing rate is increased.

Keywords

shock wave lithotripsy; cavitation bubbles; acoustic output

Please direct correspondence to: Yuri A. Pishchalnikov, Ph.D. Department of Anatomy and Cell Biology Indiana University School of Medicine 635 Barnhill Dr. MS 5055 Indianapolis, Indiana 46202−5120 USA yura@anatomy.iupui.edu 317−274−0548 FAX: 317−278−2040.

Introduction

Several recent clinical studies report that shock wave lithotripsy (SWL) is more effective in eliminating stones when SWs are delivered at a rate of ≤ 60 SW/min, compared with the typical firing rate of 120 SW/min [1-6]. This finding could mark a potentially significant change in how patients will be treated by SWL in the future. Historically, there has been great interest within the SWL community in finding ways to perform treatment as rapidly as possible [7-9]. However, slowing the firing rate breaks stones more efficiently [1-3,10-13] and also appears to cause less injury to the kidney [14,15]. But treating at a slow rate may also significantly increase treatment time, thereby extending the time the patient must be under sedation [3]. Thus, the decision to alter treatment parameters needs to be based on a solid clinical and basic science foundation, including an understanding of the acoustics mechanisms responsible for the reduced efficiency in stone breakage at faster SW rates.

Basic research on the mechanisms of SW action has shown that lithotriptor SWs can generate cavitation bubbles and that as the firing rate is increased more bubbles are produced along the SW path [13,16-18]. As gas bubbles are known to pose a substantial barrier to acoustic pulses in fluid media [19], it seems logical to expect that cavitation bubbles could pose a barrier to the propagation of SWs, and that this effect would be more pronounced as the SW rate is increased. For example, an early analysis of the acoustic output of commercial lithotriptors reported that the peak positive pressure (P +) generated by a piezoelectric lithotriptor (EDAP LT-01) was reduced by about two-fold when the SWs were delivered at a fast rate [20]. A similar result was reported in the characterization of an electrohydraulic lithotriptor (Comair Lithocut 3000) in which there was a two-fold reduction in the P + for SWs administered at 120 SW/min compared with 30 SW/min [21]. Although cavitation was not assessed in either study, it was proposed that blockage of SWs by bubbles was responsible for a reduction in the efficiency of stone breakage at faster SW rate [21]. However, more recent studies involving measures conducted in several different lithotriptors, show that at firing rates used clinically (up to 120 SW/min) SW rate has virtually no effect on the P + [12,13,22]. Such apparently contradictory findings about lithotriptor output make it difficult to fully understand the factors that can affect outcomes in SWL.

One may hypothesize that divergent results such as these could be due to differences in the cavitation fields of the experimental test systems, but this is impossible to confirm from the published accounts. Therefore, we undertook an analysis of the acoustic output of electromagnetic clinical lithotriptors operated at various firing rates under conditions in which the gas content of the water was well controlled and cavitation was monitored. The findings show that even the abundant cavitation that occurs in nondegassed water at fast firing rates failed to shield the positive-pressure phase of the SW. However, the growth of the cavitation bubbles was sufficient to attenuate the magnitude and duration of the tensile component of the shock pulse. These observations begin to define the underlying mechanism that limits the effectiveness of stone breakage when SWs are fired at fast rate.

Materials and Methods

Experiments were performed using two electromagnetic clinical lithotriptors: a standard, high-pressure lithotriptor (DoLi-50, Dornier MedTech America, Inc., Kennesaw, GA, USA) [23], and a low-pressure lithotriptor (XX-ES, Xi Xin Medical Instruments Co. Ltd, Suzhou, PRC) [5,24]. The DoLi lithotriptor has six power levels (PL1—PL6), and can deliver SWs at rates of up to 120 SW/min. The voltage of the XX-ES lithotriptor can be set continuously up to 11 kV charging potential, and most of the experiments were conducted at the recommended clinical setting of 9.3 kV. Studies were performed at the fastest rate (100 SW/min) and at the recommended clinical rate (27 SW/min) for this lithotriptor.

Measurements were conducted in an optically clear acrylic test tank filled with ~100 L of nondegassed tap water (dissolved oxygen ~99% of saturation or ~8.4 mg/L). For selected experiments, the water was degassed using a pinhole degasser run continuously, so that dissolved gas content reached a dynamic equilibrium of ~30% of saturation (2.7 mg/L) [23]. The test tank had a Mylar acoustic window (0.13 mm) for coupling with the treatment head of the DoLi (45° acoustic axis), and LithoClear gel was used as the coupling medium [25]. As the shock head of the XX-ES is above the treatment table the head was immersed directly in the water tank.

Cavitation was assessed using a high-definition NTSC frame-rate digital camcorder (HDR-HC3, Sony, Japan), and an ultrafast multiframe high-speed digital imaging system (Imacon 200, DRS Data & Imaging Systems, Inc., Oakland, NJ, USA). The camcorder was used for continuous recording of entire cavitation fields. The high-speed camera (HS-camera) was used to assess single bubble evolution after the passage of a lithotripter pulse. The HS-camera could record fourteen frames (1280 × 1024 pixels, up to 200 million frames/s) with a spatial resolution of up to 2 μm/pixel (Sigma 105 mm f/2.8 EX DG Macro Lens, Nikon PB-6 Bellows and PK11 −13 extensions). Resolution was further improved in Adobe Photoshop by subtracting images of background noise (at 75% opacity), collected without firing the lithotriptor. Bubble density in highly populated cavitation clouds (at fast rate) was assessed by counting the bubbles in the ~5 mm^2 field of view of the HS-camera. By estimating the depth of field of the HS-camera to be ~5 mm, bubble density was calculated as the number of bubbles per sampling volume (~25 mm^3).

Shock waves were measured using a fiber-optic probe hydrophone FOPH 500 (RP Acoustics, Leutenbach, Germany) positioned at the target plane specified for clinical treatment with these lithotriptors (geometric focus for DoLi; 4 cm prefocal for XX-ES [24]). Shock waves were recorded at different firing rates and voltage settings, typically in sets of 50−100 pulses, using the Fast Frame setup of the TDS 5034 Oscilloscope (Tektronix, Beaverton, OR, USA). The recorded waveforms were postprocessed with a program written in LabVIEW (National Instruments, Austin, TX, USA). The average waveforms were calculated by aligning recorded waveforms at the half amplitude of the shock fronts, as previously described [22,23].

A Tektronix P6015A high-voltage probe was used to measure the potential difference at the high voltage capacitors of the lithotriptors. The high-voltage probe was attached to the capacitors of the lithotriptors, and its readings were recorded on a Tektronix TDS 520B digitizing oscilloscope.

Results

Acoustic measurements conducted with the DoLi lithotriptor showed almost no effect of rate on the leading positive pressure phase of the SWs. A slight difference in the P + could be detected only in very dense cavitation fields that were generated in nondegassed water and at the highest power setting of the lithotriptor (Fig. 1). Even under these extreme conditions the P + at the fast rate was only ~7% less than that at a very slow rate, with a mean P + of 47.4 ±1.9 MPa at 120 SW/min vs 50.9±2.1 MPa at 5 SW/min. Although the P + and the entire leading positive- pressure phase of the SW (0−2 μs in Fig. 1) were only slightly affected, the negative-pressure phase of the pulse (~2.2−7.3 μs in Fig. 1) and trailing residual pressure oscillations (visible after ~7.3 μs in Fig. 1) were dramatically attenuated at fast rate. The peak negative pressure was reduced by ~84%, from a mean of −6.5±0.9 MPa at 5 SW/min to −1 ±0.8 MPa at 120 SW/min. The duration of the tensile component was reduced by ~80%, from 5.1±0.4 μs at 5 SW/min to 1±1 μs at 120 SW/min. The area under the waveform curve for the negative-pressure component of the pulse (integral of pressure over time) was reduced by

~98%, and the energy density of the negative-pressure phase of the waveform was reduced by 99.6%, from 80 J/m^2 at 5 SW/min to 0.3 J/m^2 at 120 SW/min.

The images collected with the camcorder provided excellent data on the relative amountof cavitation that occurred at fast versus slow SW rates. However, it should be appreciated that because the camcorder frame rate (~60 frames/s) is much slower than the overall duration of the cavitation cycle, the camcorder captured images integrated over the entire growth—collapse cycle of the cavitation bubbles. As such, these images captured bubbles at all stages throughout the cavitation cycle including their maximum expansion, and thus they overestimate the magnitude of cavitation that exists at any given point in time. For example, the frames in Fig. 1 show all visible bubbles that formed during passage of the last SW of a 10 SW series, but this is not representative of the bubble field that would exist upon arrival of the next SW. Therefore, we used multiframe high-speed photography to assess the proliferation of bubbles generated during the growth—collapse—rebound cycle and to estimate the size of bubbles at different stages throughout the cavitation cycle. Figure 2 shows a HS-camera sequence showing the response of a cavitation bubble to the passage of a lithotriptor pulse. Growth of the bubble was followed by collapse and multiple rebound—collapse cycles over time, eventually resulting in the formation of scores of minute bubbles (frame 727 μs). By ~1000 μs (data not shown), the bubbles were too small to be seen with the HS-camera. However, in previous studies we have shown that these clouds of very small bubbles remain detectable by B-mode ultrasound and, in poorly degassed water, can persist longer than a second, easily long enough to serve as cavitation nuclei when hit by subsequent SWs fired at fast rate [22]. As these tiny microbubbles (< 10 μm) constituted only a minute void fraction, we estimate < 10^{-6} for a bubble density of 1000 bubbles/cm^3, they did not noticeably affect the leading positive pressure phase of the SWs.

Acoustic measurements conducted with the XX-ES lithotriptor showed a dramatic reduction in the P + at fast rates. This was observed even when the water in the test tank was thoroughly degassed (to about 30% of saturation) and the lithotriptor was used at a power setting (9.3 kV) that generates very low acoustic pressure (P + ~20 MPa or less). The mean value for the P + (100 SWs averaging) at the fast rate was almost half that at the slow rate—12.5±1.5 MPa at 100 SW/min versus 20.9±1.1 MPa at 27 SW/min. Along with this reduction in the P +, SWs at a fast rate also showed more than a two-fold elongation of the rise time of the shock front at the fast rate (0.52 μs at 100 SW/min vs 0.23 μs at 27 SW/min, Fig. 3), as well as a reduction in the duration of the trailing negative-pressure phase of the SW (Fig. 3).

This apparent difference in the effect of rate on the P + seen with the DoLi and the XXES lithotriptors suggested the possibility of a discrepancy between the performance of these lithotriptors at different firing rates. High-voltage measurements in the charging circuits of these two lithotriptors showed that the capacitor of the DoLi was fully charged at all firing rates, but the capacitor of the XX-ES was undercharged at fast rates. At a slow firing rate (27 SW/min) the capacitor of the XX-ES was almost fully charged (98% of charging potential or 96% of energy), but at a faster rate (100 SW/min) the charging was incomplete (86% of charging potential or 74% of energy). This suggests that the effect of SW rate on P + observed with the XX-ES lithotriptor (Fig. 3) was artefactual due to the reduced electrical output of this lithotriptor at faster rates.

To better understand this potential charging artefact, tests were conducted with the XXES using different voltage settings that gave identical capacitor charge at different firing rates (Fig. 4a). Under these conditions, the leading positive-pressure phase of the SWs recorded at 27 SW/min was virtually identical to that of the SWs at 100 SW/min (Fig. 4b). However, at the fast rate the trailing negative-pressure phase was moderately attenuated (Fig. 4b). Thus, under conditions in which the XX-ES lithotriptor produced the same electrical output at different

rates, the effect of rate on the waveform was consistent with the results obtained with the DoLi lithotriptor. That is, firing rate had negligible effect on the positive-pressure phase of the SW.

Thus, measurements with the DoLi lithotriptor, in which charging of the capacitor was complete at all firing rates, showed virtually no effect of rate on the leading positive-pressure phase of the SW (Fig. 1). However, the XX-ES lithotriptor showed a significant reduction in the positive pressure phase when the firing rate was increased (Fig. 3). It was determined that this reduction in acoustic output was due to undercharging of the capacitor that supplies the SW generator (Fig. 4a), as P + was not affected by rate when the capacitor of the XX-ES lithotriptor was charged to the same level at both rates (Fig. 4b).

Discussion

The idea that cavitation might be an effective barrier to SW propagation at fast firing rates seems at first to be reasonable, as SWs fired at fast rate typically generate more bubbles than at slow rate [13,17,18]. However, the present study showed almost no effect of rate on the leading positive-pressure component of the pulse even in extremely dense cavitation fields (Fig. 1). This paradox can be understood from the following consideration.

Bubbles present upon SW arrival at the focus were typically very small (< 10 μm), smaller than could be seen with the HS-camera, and as such did not impose a barrier to the advancing SW. The small reduction in P + at fast rates was probably due to the expenditure of energy in forcing many of these tiny bubbles to collapse. Taking into account the high amplitude of P + in SWL (tens of MPa, Figs 1 and 3 [13,22-26]), one can estimate that the SW is capable of collapsing many thousands of such tiny bubbles without a noticeable reduction in P +. Thus, despite cavitation bubbles being more numerous at fast rates (Fig. 1), the effect of these very small bubbles on P + was not large.

The situation is different for the tensile component of the SW, where the energy required to drive bubble growth from, say, 5 μm to 0.5 mm (a million-fold expansion in volume), is much larger than the mechanical work needed for the advancing shock front (P +) to collapse preexisting bubbles of about the same initial size. Our previous calculations have shown that the mechanical work to expand a few dozen bubbles to a size of 1 mm would consume the entire energy of the tensile component of the SW [27]. The present experiments are in agreement with those calculations, in which the trailing negative-pressure phase was essentially eliminated when conditions (fast SW rate, high gas content) promoted extensive cavitation (120 SW/min, Fig. 1). Although proliferation of cavitation bubbles at the fast rate had minimal —to—no effect on the leading positive-pressure phase of the SW, the abundant cavitation that occurred at fast rate was sufficient to attenuate the reasonably strong (~8 MPa) positive-pressure oscillation that followed the negative tail (Fig. 1). This supports the concept of SW ”shielding” by cavitation, but also shows the time-dependence of the effect. That is, the post-tensile phase positive-pressure oscillation was attenuated at fast SW rate because at this point in time the bubbles were relatively large. The first frame in Fig. 2 (frame 7 μs) shows a bubble of ~0.25 mm in diameter. Bubbles of such a large size in sufficient number could easily quench a positive-pressure peak arriving at this time. That is, this ”shielding” effect on the trailing positive-pressure oscillation was made possible because the oscillatory positive-pressure feature was immediately preceded by the negative-pressure component of the SW that is responsible for the growth of cavitation bubbles. A similar situation exists for waveforms generated by some piezoelectric lithotripters, in which the positive-pressure shock front of the pulse is preceded by a negative-pressure precursor (Fig. 4e in [20]). This could explain the reported observation of a reduction in P + at fast firing rate with the EDAP lithotripter [20]. The leading negative-pressure phase thus increases the sizes of existing microbubbles, to absorb some of the energy of the positive wave that follows.

In theoretical studies of SW propagation in electrohydraulic lithotripsy others have predicted a reduction in positive pressure at fast rates [28-30]. However, in those studies the equilibrium radius of bubbles that would be encountered by SWs at fast firing rates far exceeded what we observed in the laboratory. The model used in those studies did not take into account that cavitation bubbles would break up on inertial collapse to form microbubbles, as we observed in the present study (Fig. 2).

Finally, our observations with the XX-ES lithotripter indicate that an apparent reduction in the P + at fast firing rates can occur due to undercharging of the capacitors that supply the SW generator. One cannot exclude the possibility that such an occurrence may have introduced an unrecognized artefact in past studies on the effect of SW rate in SWL. This current finding also serves as a reminder that lithotripter output can in some cases be different from what is expected [23].

In conclusion, although cavitation bubbles proliferate at fast SW firing rates they do not appear to pose a significant barrier to the leading positive-pressure phase of the SW. Instead, abundant cavitation fields can cause a dramatic reduction of the negative-pressure phase of the SW and can also suppress the trailing residual pressure oscillations of the pulse. The implication for lithotripsy is that reduced stone breakage at fast SW rates is not due to interference with delivery of positive pressure to the focal zone but, instead, may be due to loss of negative pressure from the SW.

Acknowledgements

The authors are grateful to Dr. XiXin Du for discussion of the charging circuit for the XX-ES lithotriptor, and to R.J. VonDerHaar for assistance during measurements with the XX-ES lithotriptor. We also thank University of Stuttgart and Dr. Eisenmenger, as well as the XiXin Co. LTD for providing the XX-ES lithotriptor, and American Kidney Stone Management for providing the DoLi lithotriptor for basic research. This study was funded by a grant from the National Institutes of Health, DK43881.

Abbreviations

SW(L), shock wave (lithotripsy); P+, peak positive pressure; SW/min, shock wave per minute; HS-camera, high-speed camera..

References

1. Pace KT, Ghiculete D, Harju M, Honey RJ. Shock wave lithotripsy at 60 or 120 shocks per minute: a randomized, double-blind trial. J Urol 2005;174:595–9. [PubMed: 16006908]
2. Madbouly K, El-Tiraifi AM, Seida M, El-Faqih SR, Atassi R, Talic RF. Slow versus fast shock wave lithotripsy rate for urolithiasis: a prospective randomized study. J Urol 2005;173:127–30. [PubMed: 15592053]
3. Yilmaz E, Batislam E, Basar M, Tuglu D, Mert C, Basar H. Optimal frequency in extracorporeal shock wave lithotripsy: prospective randomized study. Urology 2005;66:1160–4. [PubMed: 16360432]
4. Chacko J, Moore M, Sankey N, Chandhoke PS. Does a slower treatment rate impact the efficacy of extracorporeal shock wave lithotripsy for solitary kidney or ureteral stones? J Urol 2006;175:1370–4. [PubMed: 16515999]
5. Eisenmenger W, Du XX, Tang C, et al. The first clinical results of ‘wide-focus and low-pressure’ ESWL. Ultrasound Med Biol 2002;28:769–74. [PubMed: 12113789]
6. Semins MJ, Trock BJ, Matlaga BR. The effect of shock wave rate on the outcome of shock wave lithotripsy: a meta-analysis. J Urol 2008;179:194–7. [PubMed: 18001796]
7. Delius M, Jordan M, Eizenhoefer H, et al. Biological effects of shock waves: kidney haemorrhage by shock waves in dogs – administration rate dependence. Ultrasound Med Biol 1988;14:689–94. [PubMed: 3212839]

8. Ryan PC, Jones BJ, Kay EW, et al. Acute and chronic bioeffects of single and multiple doses of piezoelectric shockwaves (EDAP LT.01). J Urol 1991;145:399–404. [PubMed: 1824866]
9. Vallancien G, Aviles J, Munoz R, Veillon B, Charton M, Brisset JM. Piezoelectric extracorporeal lithotripsy by ultrashort waves with the EDAP LT 01 device. J Urol 1988;139:689–94. [PubMed: 3280830]
10. Paterson RF, Lifshitz DA, Lingeman JE, et al. Stone fragmentation during shock wave lithotripsy is improved by slowing the shock wave rate: studies with a new animal model. J Urol 2002;168:2211–5. [PubMed: 12394761]
11. Vallancien G, Munoz R, Borghi M, Veillon B, Brisset JM, Daudon M. Relationship between the frequency of piezoelectric shock waves and the quality of renal stone fragmentation. *In vitro* study and clinical implications.
12. Weir MJ, Tariq N, Honey RJ. Shockwave frequency affects fragmentation in a kidney stone model. J Endourol 2000;14:547–50. [PubMed: 11030533]
13. Pishchalnikov YA, McAteer JA, Williams JC Jr, Pishchalnikova IV, Vonderhaar RJ. Why stones break better at slow shockwave rates than at fast rates: in vitro study with a research electrohydraulic lithotripter. J Endourol 2006;20:537–41. [PubMed: 16903810]
14. Evan AP, McAteer JA, Connors BA, Blomgren PM, Lingeman JE. Renal injury during shock wave lithotripsy is significantly reduced by slowing the rate of shock wave delivery. BJU Int 2007;100:624–8. [PubMed: 17550415]
15. McAteer JA, Evan AP. The acute and long-term adverse effects of shock wave lithotripsy. Semin Nephrol 2008;28:200–13. [PubMed: 18359401]
16. Pishchalnikov YA, Sapozhnikov OA, Bailey MR, et al. Cavitation bubble cluster activity in the breakage of kidney stones by lithotripter shockwaves. J Endourol 2003;17:435–46. [PubMed: 14565872]
17. Huber P, Jochle K, Debus J. Influence of shock wave pressure amplitude and pulse repetition frequency on the lifespan, size and number of transient cavities in the field of an electromagnetic lithotripter. Phys Med Biol 1998;43:3113–28. [PubMed: 9814538]
18. Sapozhnikov OA, Khokhlova VA, Bailey MR, et al. Effect of overpressure and pulse repetition frequency on cavitation in shock wave lithotripsy. J Acoust Soc Am 2002;112:1183–95. [PubMed: 12243163]
19. Cleveland, RO.; McAteer, JA. The Physics of Shock Wave Lithotripsy.. In: Smith, AD.; Badlani, GH.; Bagley, DH., editors. Smith's Textbook on Endourology. BC Decker, Inc.; Hamilton, Ontario, Canada: 2007. p. 317-32.
20. Coleman AJ, Saunders JE. A survey of the acoustic output of commercial extracorporeal shock wave lithotripters. Ultrasound Med Biol 1989;15:213–27. [PubMed: 2741250]
21. Wiksell H, Kinn AC. Implications of cavitation phenomena for shot intervals in extracorporeal shock wave lithotripsy. Br J Urol 1995;75:720–3. [PubMed: 7613826]
22. Pishchalnikov YA, Sapozhnikov OA, Bailey MR, Pishchalnikova IV, Williams JC Jr, McAteer JA. Cavitation selectively reduces the negative-pressure phase of lithotripter shock pulses. Acoust Res Lett Online 2005;6:280–6.
23. Pishchalnikov YA, McAteer JA, Vonderhaar RJ, Pishchalnikova IV, Williams JC Jr, Evan AP. Detection of significant variation in acoustic output of an electromagnetic lithotriptor. J Urol 2006;176:2294–8. [PubMed: 17070315]
24. Evan AP, McAteer JA, Connors BA, et al. Independent assessment of a wide-focus, low-pressure electromagnetic lithotripter: absence of renal bioeffects in the pig. BJU Int 2008;101:382–8. [PubMed: 17922871]
25. Pishchalnikov YA, Neucks JS, VonDerHaar RJ, Pishchalnikova IV, Williams JC Jr, McAteer JA. Air pockets trapped during routine coupling in dry head lithotripsy can significantly decrease the delivery of shock wave energy. J Urol 2006;176:2706–10. [PubMed: 17085200]
26. Handa RK, McAteer JA, Willis LR, et al. Dual-head lithotripsy in synchronous mode: acute effect on renal function and morphology in the pig. BJU Int 2007;99:1134–42. [PubMed: 17309558]
27. Pishchalnikov YA, McAteer JA, Bailey MR, Pishchalnikova IV, Williams JCJ, Evan AP. Acoustic shielding by cavitation bubbles in shock wave lithotripsy (SWL). 17th International Symp on Nonlinear Acoustics. AIP Conf Proc 2006;838:319–22.

28. Tanguay, M.; Colonius, T. Numerical simulation of bubbly cavitating flow in shock wave lithotripsy. 4th International Symp on Cavitation; Pasadena, CA, USA. 2001. p. 1-9.

29. Tanguay, M.; Colonius, T. Progress in modelling and simulation of shock wave lithotripsy (SWL). 5th International Symp on Cavitation. Osaka, Japan. 2003. p. 1-10.number Cav03-OS-2−1−010

30. Tanguay, M. Computation of Bubbly Cavitating Flow in Shock Wave Lithotripsy. PhD Thesis. California Institute of Technology; 2003.

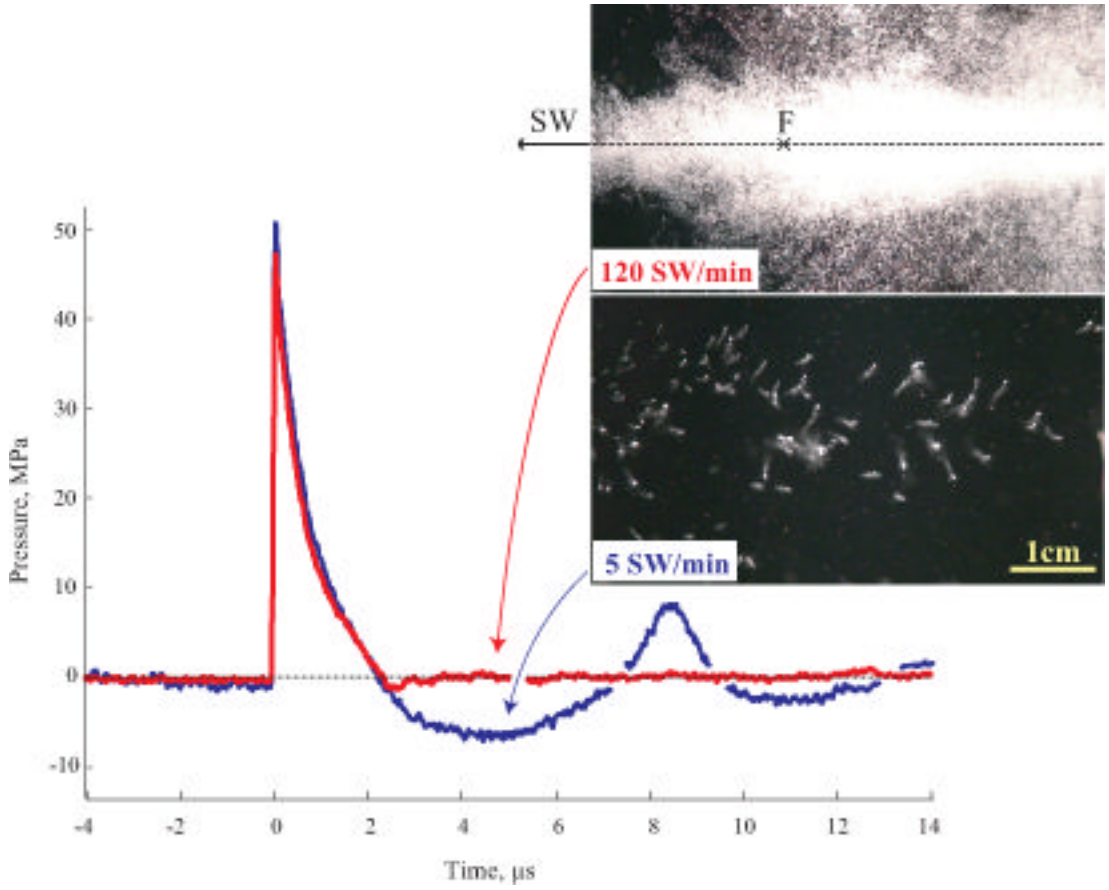

Fig. 1.

Averaged SWs (50 SWs) at two firing rates (5 SW/min and 120 SW/min) with the DoLi lithotriptor. The leading positive-pressure phase (0−2.2 μs) was only slightly affected by rate, but the negative-pressure phase (~2.2 μs−7.3μs) and trailing residual pressure oscillations (visible after ~7.3 μs) were almost completely attenuated at fast rate (120 SW/min). (These residual pressure oscillations are due to the fading oscillations of electric current in the LC circuit, where L-inductance of the coil and connective wires and C-high-voltage capacitor of the lithotriptor [22]). The inset shows representative images (10th SW at each rate) recorded with the camcorder. At 5 SW/min (bottom frame) there were only a few bubbles per cm^3. Bubble density at 120 SW/min (top frame) was up to 1000 bubbles/cm^3 (depending on the position in the field). Measurements were conducted in nondegassed water (dissolved oxygen 99% of saturation) at the highest power settings of the lithotriptor (PL6). The 100 μm glass-fiber tip of the hydrophone was positioned at the focus (F) of the lithotriptor, and is obscured from view in these images.

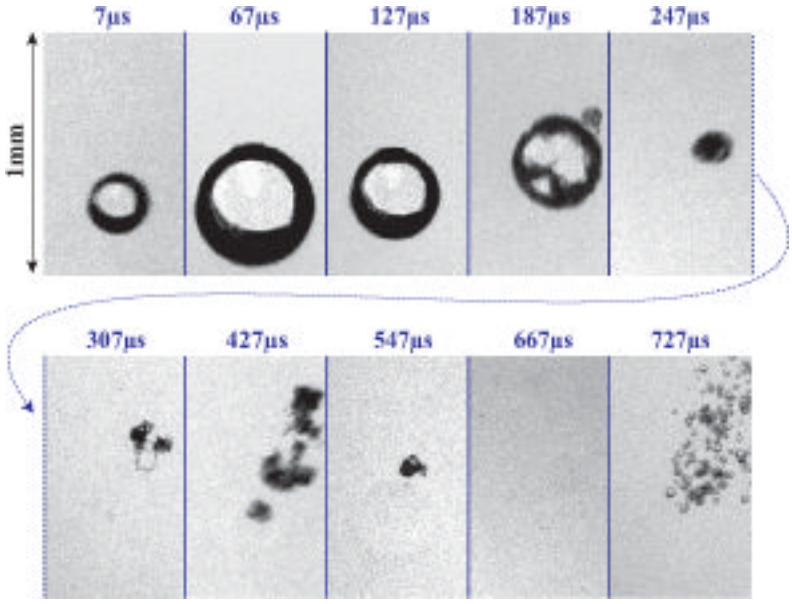

Fig. 2.

HS-camera sequence of the typical growth—collapse—rebound cycle of a cavitation bubble. The first frame (7 μs) was recorded at the end of the negative-pressure phase of the pulse (Fig. 1). Under this negative-pressure phase of the SW the bubble has grown explosively in size from below the resolution of the HS-camera (< 10 μm) to ~0.25 mm (frame 7 μs). The growth of the bubble continued after the passage of the pulse due to inertia of the surrounding liquid, reaching maximum diameter for this bubble (~0.5 mm) at ~67 μs. Then, driven by the forces of atmospheric pressure and surface tension, the bubble started to collapse, with the moment of collapse occurring between 127 and 187 μs. After this first inertial collapse, the bubble rebounded producing a microjet (187 μs). This was followed by multiple cycles of subsequent inertial collapses and rebounds (frames 247−727 μs). However, during the rebounding cycles, the bubble did not remain as a solitary bubble, but rather emerged from the inertial collapses as a cloud of microbubbles (727 μs).

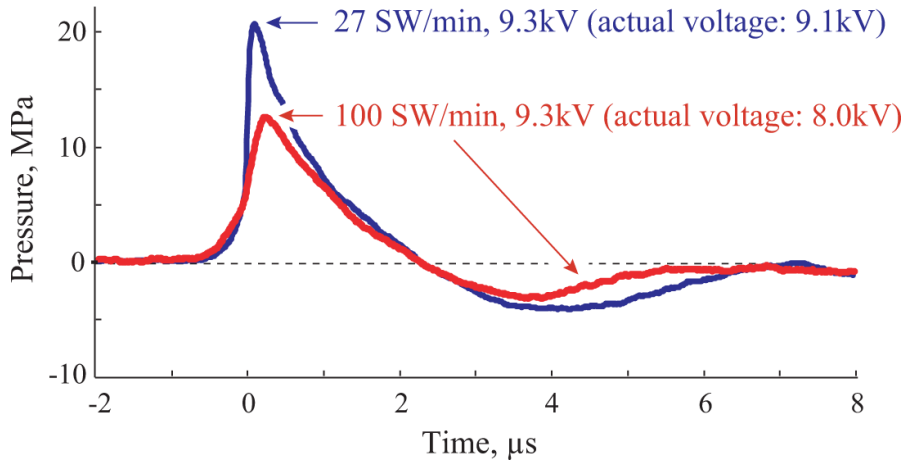

Fig. 3.

Reduced acoustic output due to the undercharging of the XX-ES lithotriptor at the fast rate. Averaged SWs (100 SWs) recorded at two firing rates imply that pressure amplitude of both the leading positive-pressure phase (0−2.2 μs) and the negative-pressure tail (2.2−7 μs) were reduced at fast rate (100 SW/min) compared with slow rate (27 SW/min). However, the actual kV values were different at the two firing rates.

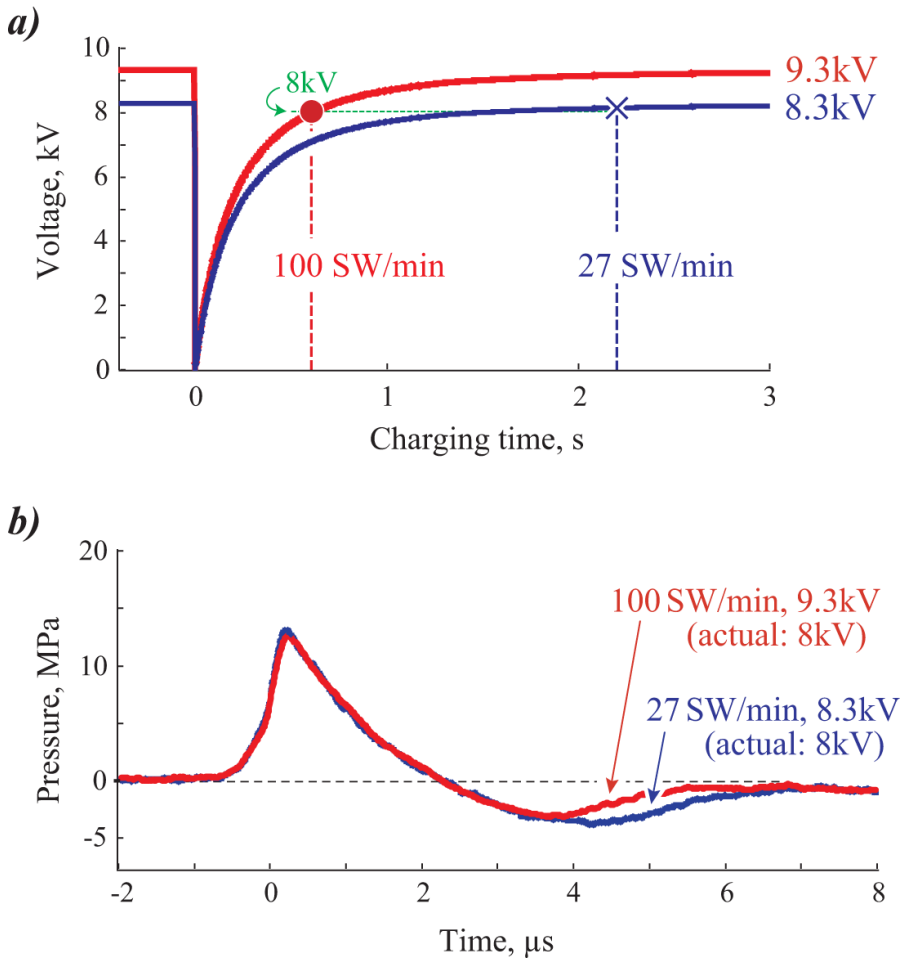

Fig. 4.

Retest of XX-ES lithotriptor using voltage settings to yield identical charging potentials at slow and fast firing rates. ***a)***— Potential difference at the high voltage capacitor at 8.3 kV and 9.3 kV voltage settings of the XX-ES lithotriptor. After the discharge (at 0 s), the capacitor began to accumulate electric charge, exponentially approaching the charging potential of the lithotriptor. The capacitor was almost fully charged at 27 SW/min (charging time 2.2 s), and was undercharged at faster rates, e.g. 100 SW/min (charging time 0.6 s). ***b)***— Averaged SWs (100 SWs) recorded at two rates under conditions that provide the same electrical output of the XX-ES lithotriptor (marked by a dot and a cross in the charging curves of frame ***a***). When the charge of the high voltage capacitor was the same, the leading positive-pressure phase (0 −2.2 μs) was unaffected by firing rate. The negative-pressure tail (2.2−7μs) was reduced at fast rate (100 SW/min) compared with slow rate (27 SW/min).